Analytica Chimica Acta xxx (2016) 1–8

Contents lists available at ScienceDirect

Analytica Chimica Acta

journal homepage: www.elsevier.com/locate/aca

Novel CeO_2–CuO-decorated enzymatic lactate biosensors operating in low oxygen environments

Aytekin Uzunoglu [a, *], Lia A. Stanciu [a, b]

[a] School of Materials Engineering, Purdue University, 701 West Stadium Avenue, West Lafayette, IN 47907, USA
[b] Weldon School of Biomedical Engineering, Purdue University, 206 South Martin Jischke Drive, West Lafayette, IN 47907, USA

HIGHLIGHTS

- Here, we described the use of CeO_2–CuO nanoparticles to address the oxygen dependence challenge of first generation amperometric lactate biosensors.
- The use of CeO_2–CuO mixed metal oxide acted as an oxygen buffer on the sensing platform in oxygen-depleted buffer solution.
- The false results associated with the depletion of oxygen tension in PBS solution were eliminated.

GRAPHICAL ABSTRACT

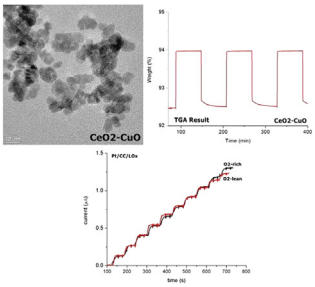

ARTICLE INFO

Article history:
Received 24 September 2015
Received in revised form
26 December 2015
Accepted 30 December 2015
Available online xxx

Keywords:
Amperometric lactate biosensors
Ceria-based metal oxides
Oxygen storage capacity
Oxygen dependency
Lactate oxidase

ABSTRACT

The detection of the lactate level in blood plays a key role in diagnosis of some pathological conditions including cardiogenic or endotoxic shocks, respiratory failure, liver disease, systemic disorders, renal failure, and tissue hypoxia. Here, we described for the first time the use of a novel mixed metal oxide solution system to address the oxygen dependence challenge of first generation amperometric lactate biosensors. The biosensors were constructed using ceria-copper oxide (CeO_2–CuO) mixed metal oxide nanoparticles for lactate oxidase immobilization and as electrode material. The oxygen storage capacity (OSC, 492 μmol-O_2/g) of these metal oxides has the potential to reduce the oxygen dependency, and thus eliminate false results originated from the fluctuations in the oxygen concentration. In an effort to compare the performance of our novel sensor design, ceria nanoparticle decorated lactate sensors were also constructed. The enzymatic activity of the sensors were tested in oxygen-rich and oxygen-lean solutions. Our results showed that the OSC of the electrode material has a big influence on the activity of the biosensors in oxygen-lean environments. While the CeO_2 containing biosensor showed an almost 21% decrease in the sensitivity in a O_2-depleted solution, the CeO_2–CuO containing electrode, with a higher OSC value, experienced no drop in sensitivity when moving from oxygen-rich to oxygen-lean conditions. The CeO_2–CuO decorated sensor showed a high sensitivity (89.3 ± 4 μA mM^{-1} cm^{-2}), a wide linear range up to 0.6 mM, and a low limit of detection of 3.3 μM. The analytical response of the CeO_2–CuO decorated sensors was studied by detecting lactate in human serum with good selectivity and reliability. The results revealed that CeO_2–CuO containing sensors are promising candidates for continuous lactate detection.

* Corresponding author.
E-mail addresses: auzunogl@purdue.edu, aytekingyte@gmail.com (A. Uzunoglu).

http://dx.doi.org/10.1016/j.aca.2015.12.044
0003-2670/

1. Introduction

An increased lactate level in blood is used to diagnose a higher risk of morbidity both in emergency and surgical operations [1,2]. Moreover, it is known that an increased lactate level is associated with some pathological conditions such as cardiogenic or endotoxic shocks, respiratory failure, liver disease, systemic disorders, renal failure, and tissue hypoxia [3–6]. The first protocol to measure the lactate concentration in blood was introduced in 1886, and relied on the collection of a large quantity of blood sample (100–200 ml) and labour intensive steps [1]. In addition to these challenges, it required several days to complete the measurement [1]. Since then, intensive effort has been devoted to construct small sized devices with shorter turnaround time to measure the blood lactate level using minimal amount of sample. The technological advances in the last couple of decades enabled scientists to invent new methods to detect the lactate concentration less than 2 min [7]. Although the concentration of lactate can be measured using various methods including liquid and gas chromatography, optical analysis, chemical oxidation, and enzymatic oxidation, these methods are complex, require pretreatment and expertise [6,8]. Therefore, construction of inexpensive and simple lactate biosensors with high sensitivity and selectivity, a low limit of detection, and a fast response time, which requires no expertise has gained great attention in the last couple of decades.

The use of amperometric biosensors is an alternative method to conventional approaches for the detection of lactate level in blood [3,9]. Since amperometric biosensors have several advantages over the conventional methods, they have been studied extensively. The detection of lactate using an amperometric enzyme biosensor requires the application of a potential between working and reference electrodes [3]. The main components of the working electrode are enzyme and catalyst layers, which take part in oxidations of lactate and hydrogen peroxide, respectively. To date, lactate oxidase is the most commonly used enzyme as the biological component in enzymatic lactate biosensors [6]. Lactate oxidase catalyses the oxidation of lactate as described Eq. (1) [3].

$$\mathrm{L-Lactate} + \mathrm{O_2} \xrightarrow{LOx} \mathrm{pyruvate} + \mathrm{H_2O_2} \quad (1)$$

The produced H_2O_2 is then oxidized on the catalyst surface according to Eq. (2) at a certain potential [3].

$$\mathrm{H_2O_2} \rightarrow \mathrm{O_2} + 2\mathrm{H^+} + 2\mathrm{e^-} \quad (2)$$

Since the amount of lactate is proportional to H_2O_2 generated by lactate oxidation, its concentration is used to determine the lactate concentration by measuring the current generated from the oxidation of hydrogen peroxide [3,10]. As indicated Eq. (1), oxygen is utilized as the physiological electron acceptor for lactate oxidation reaction. Therefore, the detection of lactate level using these biosensors is highly dependent on the oxygen concentration. On the other hand, oxygen concentration in blood is subject to fluctuations resulting in errors in measured lactate concentrations [11]. Moreover, oxygen deficiency in the blood sample deteriorates the detection range of the sensors [12]. The inadequate oxygen level cannot sustain the oxidation of lactate; thus, fluctuations in the oxygen concentration hinder accurate detection of lactate level. To eliminate the oxygen dependency problems in electrochemical sensors, some approaches have been proposed including the use of two dimensional cylindrical electrodes [13], mass transport limiting films [13,14], and tailoring the electrode surface with oxygen-rich materials [15]. In addition to the modification of electrode using one of the approaches listed above, some authors substituted lactate oxidase with lactate dehydrogenase (LDH) which does not require oxygen as an electron acceptor [3]. On the other hand, the replacement of lactate oxidase with lactate dehydrogenase enzyme requires the immobilization of coenzymes (NADH or NADPH), which enables the electron transfer between enzyme and electrode surface [3]. Since the immobilization of coenzymes makes the sensor construction more complicated in terms of enzyme immobilization and regeneration, publications that used lactate oxidase outnumbered those that used lactate dehydrogenase [3]. In addition, it was reported that lactate dehydrogenase based biosensors showed lower sensitivity compared to the biosensors with lactate oxidase [3,6]. With the introduction of the second generation biosensors, oxygen was replaced with a synthetic electron acceptor known as artificial mediator to make the electrodes oxygen independent [12]. In the case of an artificial mediator, although higher electron transfer rates and lower working potentials can be achieved, the presence of the mediator in the enzyme layer may impair the enzyme stability by creating a toxic environment [3]. Thus, choosing the right mediator, which is not detrimental to enzymatic activity is a key step in the construction of second-generation biosensors. Moreover, the immobilization and stability of the artificial mediator are also challenges to be dealt with [11,16]. In summary, most of the methods used to eliminate the oxygen deficiency related errors in the sensor response pose new problems including sensitivity, selectivity, and stability, require more complex preparation methods and hinder the miniaturization of sensors [17]. Thus, new approaches are on demand to address the oxygen dependence challenge of first generation enzymatic sensors.

In recent years, the use of metal oxide nanoparticles has attracted great interest in several applications such as catalysis, sensors, electronic materials, and environmental materials due to their unique physical, catalytic, and chemical properties [18,19]. Since the properties of the metal oxide nanoparticles are highly dependent upon their size and morphology, they offer vast range of properties for various applications [20]. Their biocompatible nature, enhanced electron-transfer kinetics and strong adsorption capability make them promising materials for the immobilization of biomolecules in biosensing applications [21,22]. Among various metal oxides, ceria has been used in many applications including catalysis, solid oxide fuel cells [23], sensors [24], oxygen permeable membranes [25], glass polishing [26], ultraviolet adsorption [27], and biotechnology [19,28]. Its high ionic conductivity, biocompability, high surface area, high isoelectric point, and catalytic properties generated great deal of interest for biosensor applications [22,29]. Apart from these properties, the unique redox properties of ceria, also known as oxygen storage capacity (OSC), make it an important technological material for many applications [30]. Since cerium (Ce) can exist in two oxidation states, Ce^{4+} and Ce^{3+}, it forms two stable oxide species which are CeO_2 and Ce_2O_3 [31]. By a reversible shift between +4 and +3 oxidation states, ceria releases and uptakes oxygen under oxygen lean and oxygen rich environments, respectively. The reversible redox property of CeO_2 has been exploited extensively as an oxygen buffer material for automotive applications in particular three-way catalysis [30,31]. Much effort has been directed toward preparing new ceria-based nanomaterials with enhanced OSC. It is known that the OSC of ceria is strongly dependent on the specific surface area and oxygen defect concentration in the structure [31,32]. Our previous work showed that the modification of ceria with other metal oxides such as CuO, TiO_2, and ZrO_2 is an effective way to significantly enhance the OSC of ceria [31]. The introduction of ZrO_2 into the CeO_2 lattices, for example, gave rise to the number of oxygen defects in the ceria structure, which in turn enhanced the OSC.

Recently, our group showed that the oxygen deficiency formed in the enzyme layer of amperometric lactate biosensors can be

Please cite this article in press as: A. Uzunoglu, L.A. Stanciu, Novel CeO_2–CuO-decorated enzymatic lactate biosensors operating in low oxygen environments, Analytica Chimica Acta (2016), http://dx.doi.org/10.1016/j.aca.2015.12.044

eliminated by the incorporation of ceria nanoparticles into the enzyme layer [33]. Up to now, few studies have reported the use of ceria as an oxygen buffer in the enzyme layer of amperometric first generation sensors [18,34,35]. In this paper, lactate oxidase enzymes were immobilized on a novel mixed metal oxide system (CeO_2–CuO) with an enhanced OSC for the first time to improve the performance of the lactate sensors in both oxygen-rich and lean environments. The CeO_2–CuO system was chosen for lactate oxidase immobilization and as an electrode material since in our previous report it was shown that this mixed metal oxide system had superior OSC and higher surface area than CeO_2–ZrO_2, CeO_2–TiO_2 mixed metal oxides [31]. The results revealed that the enhanced OSC of CeO_2–CuO mixed metal oxide nanoparticles eliminated the false results associated with oxygen deficiency.

2. Experimental

2.1. Materials

$Ce(NO_3)_3.xH_2O$ (99.999%), $N_2O_7Zr.xH_2O$ (99.0%), $CuN_2O_6.xH_2O$ (99.999%), nafion solution (5 wt%), LOD (lyophilized powders containing 40 U mg^{-1} solid, from Pediococcus species), L-lactic acid, and PBS buffer solution (0.01 M, pH = 7.4) were purchased from Aldrich. NH_4OH (28–30%) was obtained from Science Lab. Lactate assay kit (MAK064) was purchased from Sigma-Alrich. The chemicals were used as received.

2.2. Preparation and characterization of mixed metal oxides

Mixed metal oxide powders were synthesized via a room temperature coprecipitation method. Firstly, 0.1 M stock solution of each precursor was prepared by dissolving the starting materials in deionized water. To prepare CeO_2–CuO mixed metal oxide, 75 ml of cerium and 25 ml of copper precursor stock solutions were mixed in a beaker and sonicated to obtain a homogeneous solution. Subsequently, 4 M, 25 ml of fresh NH_4OH solution was added drop wise to the precursor mixture under vigorous stirring. The solution was kept stirring for one more hour and left for ageing overnight at room temperature. After the room temperature ageing, the precipitated metal oxide particles were separated from the solution by centrifuge, dried at 100 °C overnight and calcined at 500 °C for 5 h under ambient atmosphere.

X-Ray diffraction (XRD) patterns of the samples were recorded using a Bruker D8 Focus X-Ray Diffractometer with Cu Kα (λ = 0.15406 nm) radiation. The XRD experiments were conducted at the scan rate of 4° min^{-1} over 2θ values between 20° and 70°. Scherrer equation was implemented to calculate the average crystalline size. The particle size and morphology of the samples were studied using an FEI-Tecnai Transmission electron microscopy (TEM) operating at 200 kV.

The specific surface area of the samples was measured using N_2 adsorption-desorption analysis at −196 °C based on multipoint Brunauer-Emmit-Teller (BET) theory. A TriStar 300 was employed to conduct physisorption experiments. All the samples were degassed at 300 °C for 3 h prior to N2 physisorption.

A SDT 2960 (from TA Instruments) Differential-Thermal analyzer was used to determine the OSC of the prepared mixed metal oxide systems. 50 mg of the sample was exposed to reductive (5% H_2/Ar) and oxidative (synthetic air) environments at 600 °C, alternatively. The change in the sample mass under alternating reductive and oxidative environments was considered to total OSC of the samples (μmolO_2/g powder).

2.3. Construction and characterization of lactate biosensors

Prior to the construction of biosensors, a standard Pt electrode with the diameter of 3 mm was polished using 3 μm and 0.05 μm Al_2O_3 slurries, respectively. 4 μl of mixed metal oxide containing PBS solution (10 mg metal oxide/ml PBS) was dropped on the polished Pt surface, and then left for drying. After modification of Pt surface with metal oxide particles, 2 U of LOD solution was dropped on the electrode surface. The outer layer of the electrode was covered with a thin nafion layer that acted to eliminate the enzyme leakage and exclude common interfering species via electrostatic repulsion.

The electrochemical experiments were conducted using a three-compartment electrochemical half-cell (BASI, West Lafayette, IN) consisting of a Pt wire and an Ag/AgCl electrode as counter and reference electrodes, respectively. All the electrochemical experiments were carried out at room temperature in 0.01 M PBS solution (pH = 7.4). Oxygen lean PBS solution was created by purging argon for 5 min. Argon gas was fed to the surface of the solution during the experiments to maintain the oxygen depleted solution.

3. Results

3.1. Characterization of metal oxide nanoparticles

The comprehensive characterization of the prepared metal oxide nanoparticles is reported in our previous work [31]. Here, the physical characterization of the samples is shown briefly for the sake of the integrity of this paper. The XRD results of the samples (Fig. 1) indicated that the prepared metal oxide samples had the fluorite structure with the peaks appeared at 28.54°, 33.16°, 47.50°, and 56.36° (JCPDS 34-0394). The XRD peaks indicated with asterisks (*) in Fig. 1 belong to MgO crystal structure, which was used as an internal standard. With the introduction of Cu^{2+} ions into the CeO_2 lattice, no obvious change was observed in the location of the peaks suggesting that the samples had similar lattice parameters. On the other hand, the broadening of the peaks displayed that the incorporation of second metal oxide resulted in a decrease in the average crystalline size. Table 1 summarizes the average crystalline size and lattice parameters of the samples. It was seen that CeO_2–CuO mixed metal oxide nanoparticles has smaller crystalline sizes compared to CeO_2. The CeO_2–CuO system did not show the formation of the secondary phase, suggesting the formation of solid solution.

The BET surface area of the samples was found to be 55.7 and 97.3 m^2/g for CeO_2 and CeO_2–CuO respectively. The introduction of

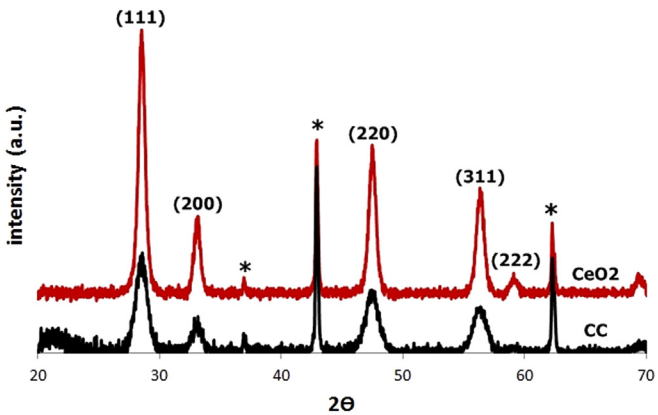

Fig. 1. X-Ray diffraction patterns of the prepared samples (CC: CeO_2–CuO).

Please cite this article in press as: A. Uzunoglu, L.A. Stanciu, Novel CeO_2–CuO-decorated enzymatic lactate biosensors operating in low oxygen environments, Analytica Chimica Acta (2016), http://dx.doi.org/10.1016/j.aca.2015.12.044

Table 1
Crystallite size, lattice parameter, and BET surface area of the samples.

Sample	Definition	BET surface area (m^2/g)	Lattice parameter (Å)	Crystalline size (nm)	Average mass change (mg)	Total OSC (μmol-O_2/g powder)
CeO_2	CeO_2	55.7	5.41	13.0	0.16	93
CC	CeO_2–CuO	97.3	5.41	7.2	0.72	492

Cu^{2+} ions into the ceria lattice enlarged the surface area up to 97.3 m^2/g. The measured specific area of the samples is shown in Table 1. The nitrogen adsorption-desorption isotherms indicated that the samples had a mesoporous structure (Fig. S1). It was seen that the obtained specific surface area values are fully compatible with the average crystalline size values. The TEM images of the samples shown in Fig. S2 indicated that the mixed metal oxide systems showed smaller particle sizes than ceria powders, which confirms the XRD results. Although the formation of solid solution resulted in a decrease in the particle size, similar particle shape and morphology were observed for both samples.

The TGA results showed that CuO containing sample had the highest mass change under the alternating environment. The mass change in the TGA profile (Fig. S3) shows the amount of oxygen, which is released and adsorbed under reductive and oxidative environments, respectively. The OSC values of the samples are listed in Table 1. The introduction of Cu^{2+} ions into the ceria lattice increased the OSC more than 5 times compared to pristine ceria. The increase in the number of oxygen defects in the ceria structure, the enlarged surface area, and strong interaction between Ce^{4+} and Cu^{2+} cations play a key role in the significant increase in the OSC of CeO_2–CuO mixed metal oxide [31,32]. In addition, the strong interaction between these cations increases the OSC by weakening the metal-oxygen bonds [32].

3.2. Electrochemical characterization of the constructed biosensors

The electrocatalytic activity of the prepared electrodes towards lactate was studied using cycling voltammetry conducted at the scan rate of 10 mV s^{-1} in PBS solution. When 5 mM lactate was added into PBS solution, an oxidation peak appeared, which belongs to the oxidation of H_2O_2 produced by enzymatic lactate reaction. The CV graphs are shown in Fig. 2. The results indicated that all of the constructed sensors had the capability of lactate detection at around 0.6 V. The effect of the scan rate on the performance of the sensors were investigated at scan rates ranging from 10 to 450 mV s^{-1}. As shown in Fig. S4, the oxidation peak current showed a linear relationship with the scan rate indicating that the oxidation of H_2O_2 on the surface of the prepared sensors is a surface-controlled electrochemical reaction.

The optimum working potential of the constructed sensors for the detection of lactate was determined by measuring the response current of the sensors towards 5 mM lactate in PBS at various working potentials ranging from 0.3 to 0.9 V (Fig. 2d). Low response currents were obtained at the working potentials below 0.4 V. When the applied potential was increased up to 0.6 V, a sharp increase in the current was observed. Although further increase in the applied voltage gave rise to the response current up to 0.7 V, the increment was not as dramatic as those obtained at 0.6 V. The working potential of 0.6 V was used for further experiments because the performance of the sensor did not increase significantly at a higher working potential.

The amperometric response of the constructed lactate sensors were measured by the successive addition of 50 μM lactate in PBS solution under a constant stirring throughout the experiment. The *i-t* graphs of the sensors are shown in Fig. 3a. The results showed that CeO_2 and CeO_2–CuO containing sensors showed much faster response time (<10s) than Pt/LOx sensor, suggesting that the decoration of the electrode surface with nanoparticles enhanced the catalytic activity of the sensing platforms. Fig. 3b shows the amperometric performance of the sensors to the successive addition of lactate into the PBS solution at the working potential of 0.6 V. The performance of Pt/LOx biosensors was much lower compared with the nanoparticle based sensors. The increase in the activity of the biosensors by the incorporation of ceria based nanoparticles may be attributed to the high surface area of the metal oxides, which favoured enzyme immobilization. In addition, the easier electron transfer process between the enzyme and electrode surface, catalytic activity of ceria towards H_2O_2, and the increase in the catalytic surface area may be all reasons behind the increase in the performance of the sensors. While the linear range of Pt/LOx was found to be between 20 and 200 μM, the CeO_2 and CeO_2–CuO nanoparticle decorated sensors showed a linear range between 20 and 600 μM. The obtained sensitivity values were 40.5 ± 5, 105.9 ± 7, and 89.3 ± 4 μA mM^{-1} cm^{-2} for Pt/LOx, Pt/CeO_2/LOx, and Pt/CC/LOx, respectively. It was observed that the incorporation of Cu^{2+} ions into the ceria lattice to increase the number of oxygen defects impaired the catalytic activity of the metal oxide particles. It is noteworthy that the presence of Cu^{2+} ions into the CeO_2 lattice resulted in a dramatic increase in the specific surface area (Table 1). In contrast to the increase in the surface area, the lower performance of CuO containing sensor is due to the difference in the catalytic activity of CeO_2 and CuO towards the oxidation of H_2O_2. Our preliminary work, which is not shown in this article, confirmed the lower catalytic activity of CuO than that of CeO_2 towards H_2O_2.

Herein, we aimed to reduce the oxygen deficiency related errors in the sensor response by decorating the surface of the electrode with nanomaterials with high redox properties (OSC). The performance of the constructed sensors in O_2-rich and -lean conditions were examined to determine the drop in the sensitivity and the change in the linear range. The amperometric response of the sensors to the successive addition of 20 μM lactate in oxygen-rich and -lean environments are shown in Fig. 4a–c. It was seen that nanoparticle-free sensor (Pt/LOx) showed a sharp decrease in its sensitivity when exposed to oxygen-lean condition. Since there is some dissolved oxygen in the enzyme layer and PBS solution, the sensor showed a response to the addition of lactate in O_2-depleted PBS. On the other hand, the obtained was very low and no linearity between the response current and lactate concentration was observed from the graph. When the surface of the sensor was modified with ceria nanoparticles, the drop in the sensitivity between O_2-rich and -lean conditions decreased and a better response-concentration graph was obtained. The reduction in the performance drop between Pt/LOx and Pt/CeO_2/LOx resulted from the OSC of ceria nanoparticles. It is speculated that CeO_2 is reduced to Ce_2O_3 by the enzymatically produced H_2O_2, as shown in Eqs. (3) and (4). Thus, the reduction of ceria by H_2O_2 produced oxygen and water in the enzyme layer [34,35]. The generated O_2 in the enzyme layer was used to sustain the enzymatic reaction in oxygen-lean conditions, which resulted in a lower performance drop compared to Pt/LOx. The introduction of CeO_2–CuO nanoparticles, which has much higher OSC compared to pristine CeO_2, showed almost no drop in the sensitivity depending on the O_2

Please cite this article in press as: A. Uzunoglu, L.A. Stanciu, Novel CeO_2–CuO-decorated enzymatic lactate biosensors operating in low oxygen environments, Analytica Chimica Acta (2016), http://dx.doi.org/10.1016/j.aca.2015.12.044

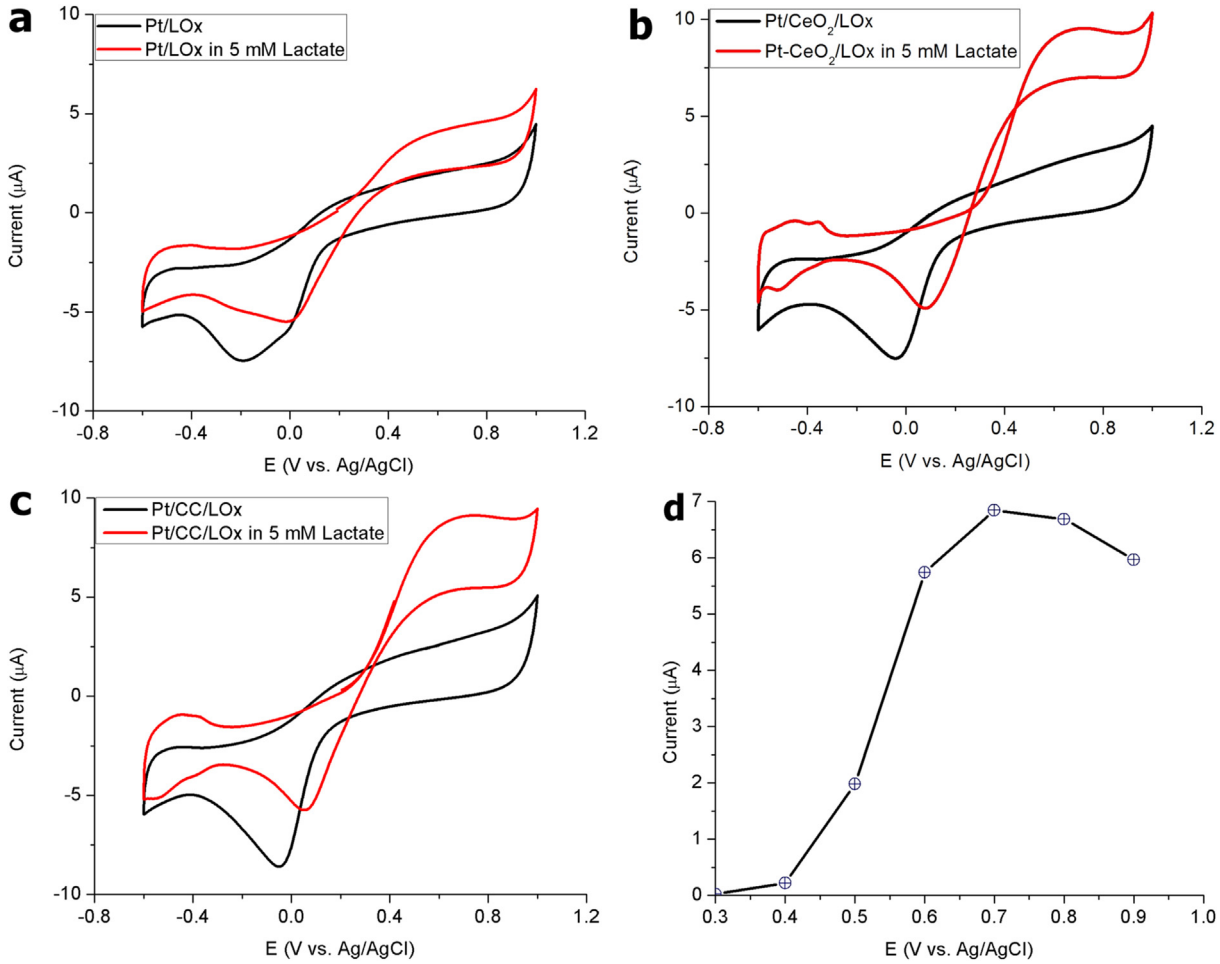

Fig. 2. (a–c) Cyclic voltammetry results of the sensors in the absence and presence of 5 mM lactate in PBS at the scan rate of 10 mV s^{-1}, (d) response current of Pt/CeO_2/LOx to the addition of 5 mM lactate as a function of applied voltage.

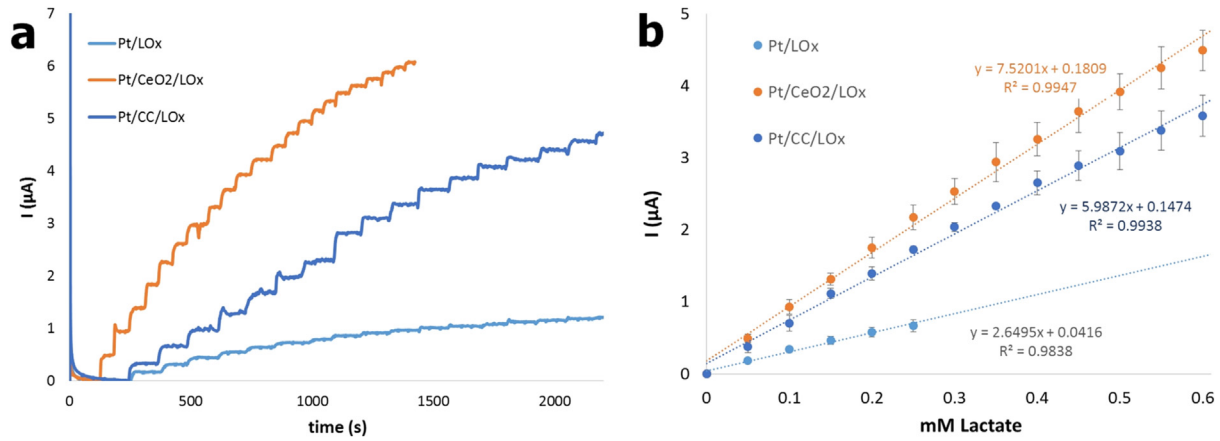

Fig. 3. (a) Current-time curves of the constructed sensors obtained from the successive addition of 50 μM lactate into PBS at the applied potential of 0.6 V, (b) Corresponding current-concentration curves.

concentration in PBS solution (Fig. 4c). This is attributed to the very high redox capacity of CuO modified CeO_2. The error values (%) calculated from the sensitivity drops when moving from oxygen-rich to oxygen-lean conditions are shown in Fig. 4d. The obtained error values were 28.7 ± 8, 20.9 ± 2, and −1.5 ± 2.9% for Pt/LOx, Pt/CeO_2/LOx, and Pt/CC/LOx, respectively (Table S1, n = 3). The results indicated that although Pt/LOx and Pt/CeO_2/LOx sensors are capable of detection of lactate in oxygen-lean environments, the use of these sensors is not practical due to their susceptibility to high degree of errors resulted from fluctuations in O_2 concentration. To detect the analyte concentration with confidence in environments with fluctuating O_2 concentrations, not only the

Please cite this article in press as: A. Uzunoglu, L.A. Stanciu, Novel CeO_2–CuO-decorated enzymatic lactate biosensors operating in low oxygen environments, Analytica Chimica Acta (2016), http://dx.doi.org/10.1016/j.aca.2015.12.044

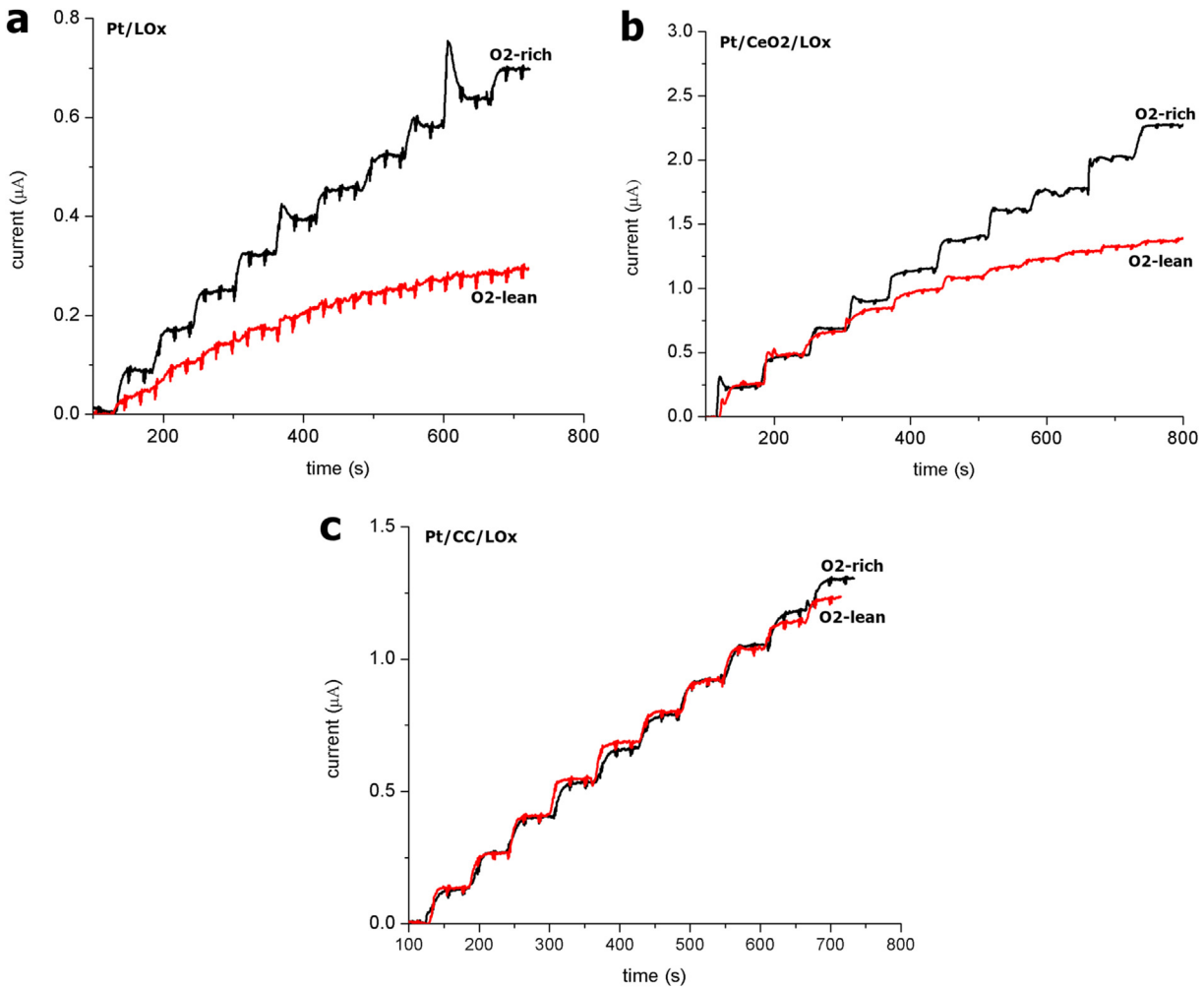

Fig. 4. Current-time curves of (a) Pt/LOx, (b) Pt/CeO_2/LOx, (c) Pt/CeO_2–CuO/LOx in the O_2-rich and –lean environments.

detection capability but also insusceptibility of sensitivity to any fluctuations in O_2 concentration is required. Our results showed that the sensor prepared with electrodes that were decorated with CeO_2–CuO mixed metal oxide nanoparticles had the capability to detect lactate under O_2-lean environments with no drop in sensitivity.

$$L - Lactate + O_2 \xrightarrow{LOx} pyruvate + H_2O_2 \quad (3)$$

$$2CeO_2 + H_2O_2 \rightarrow Ce_2O_3 + O_2 + H_2O \quad (4)$$

Fluctuations in the oxygen tension in the environment also affect the linear range of the sensors [12]. In other words, oxidase enzyme based sensors display a narrower linear range due to the oxygen deficit under O_2-lean conditions. The linear range and the limit of detection values of the constructed sensors under oxygen-rich and -lean conditions are listed in Table 2. The results showed that the linear range of the constructed sensors decreased significantly in oxygen-lean conditions. Although CeO_2–CuO decorated sensors showed promising results in terms of sensitivity, the upper limit of linearity underwent a significant drop. It is interesting to note that Pt/LOx and Pt/CeO_2/LOx sensors showed the same upper concentration dependent limit regardless of the OSC property of ceria nanoparticles. This suggests that at relatively high lactate concentrations, the OSC of ceria based materials could not supply enough oxygen to sustain the enzymatic lactate oxidation. Indeed, the reduction of the upper limit of the linear range remains as a challenge to be addressed. No significant change was observed in the limit of detection of all sensors regardless of the modification of the sensing platform with ceria-based nanoparticles (Table 2). The low limit of detection values were obtained for all sensors in both oxygen-rich and -lean conditions. The response of the constructed Pt/CC/LOx sensor to the addition of 1 and 5 μM lactate is shown in Fig. S5. It was seen that the sensor showed the capability of the detection of 5 μM lactate. The long term stability of Pt/CC/LOx was evaluated by measuring the response current of the sensor toward 5 mM lactate periodically. The sensor was stored at 4 °C in PBS solution to decelerate the enzyme denaturation and leakage. It's been observed that the sensor retained 64% of its original performance after 14 days. The repeatability of the fabrication process was determined by measuring the sensitivity of multiple Pt/CC/LOx sensors (n = 3). The RSD of the sensitivity values obtained from three independent sensors was found to be 6.3% indicating a good repeatability of the fabrication process. The reproducibility of the analytical response of a Pt/CC/LOx sensor was evaluated by comparing the response of the sensors towards the addition of 0.5 mM lactate. A RSD of 6.7% was obtained after 24 independent experiments and no sensible drop in the analytical response observed (Fig. S6), suggesting good reproducibility and stability of the analytical response of the constructed sensors.

Please cite this article in press as: A. Uzunoglu, L.A. Stanciu, Novel CeO_2–CuO-decorated enzymatic lactate biosensors operating in low oxygen environments, Analytica Chimica Acta (2016), http://dx.doi.org/10.1016/j.aca.2015.12.044

Table 2
Linear range and limit of detection values of the sensors in O_2-rich and -lean environments.

Biosensor	Linear range in O_2- saturated PBS (μM)	LOD in O_2- saturated PBS (μM)	Linear range in O_2-depleted PBS (μM)	LOD in O_2- depleted PBS (μM)
Pt/LOx	20–250	6.6	20–120	9.9
Pt/CeO_2/LOx	20–600	1.65	20–120	2.0
Pt/CC/LOx	20–600	3.3	20–200	2.97

LOD: limit of detection.

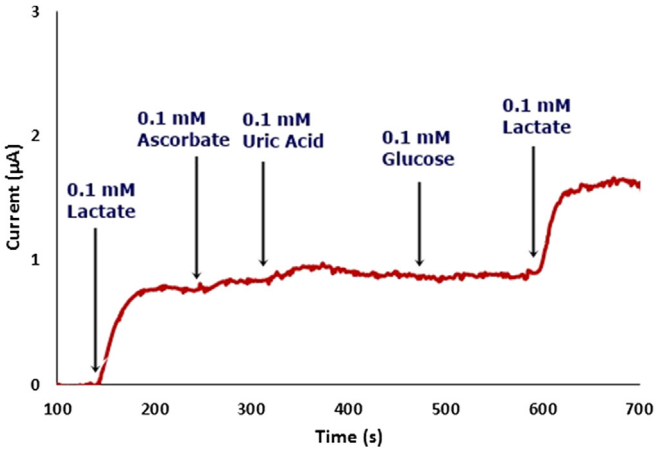

Fig. 5. Effect of common interferants on the biosensor response.

Table 3
Detection of lactate in 10 times diluted human serum.

Experiment	Before spike (μM)	Spiked (μM)	After spike (μM)	Recovery (%)
1	50	100	146	95.7
2	53	100	163	110
3	54	100	147	93

The effect of electroactive interferants on the electrochemical performance of Pt/CC/LOx was evaluated by the addition of 0.1 mM uric acid (UA), ascorbic acid (AA), and glucose into PBS solution at the working potential of the sensor. It is known that these electroactive species co-exist with lactate in blood and lead to significant changes in the response current of electrochemical sensors [36]. The results of the selectivity experiments (Fig. 5) revealed that the lactate biosensor did not experience any change in response upon exposure to these interferants. It is noteworthy that the interference-free detection of lactate in the presence of most common interfering species was made possible by the presence of negatively charged nafion, which excluded the negatively charged interferants via electrostatic repulsion.

To evaluate the practical applicability of the constructed sensor, the recovery of lactate injected into human serum was calculated based on previously reported protocols [37]. Human serum diluted 10 times was used to mimic detection in real samples. The response current of Pt/CC/LOx increased by 0.18 ± 0.006 μA when the sensor was exposed to the diluted human serum. The lactate level in human serum was calculated as 0.52 ± 0.02 mM, which is in agreement with the level of lactate in human serum determined using a colorimetric lactate assay kit (0.51 ± 0.06 mM). For the spike measurement, a known amount of lactate (0.1 mM) was injected into the sample. The spike test results and the corresponding recovery values are shown in Table 3. The recovery values were found to be between 93 and 110% showing the applicability of the sensors in real systems.

The performance of the Pt/CC/LOx sensor was compared with the already reported lactate sensors in the literature. The constructed sensor showed a low limit of detection (3.3 μM), a high sensitivity (89.3 ± 4 μA mM^{-1} cm^{-2}), and a wide linear range (up to 0.6 mM). The performance of the fabricated sensors are comparable or even better than the already existing electrochemical lactate sensors (Table 4).

4. Conclusion

In this work, we aimed to eliminate the errors in the detection of lactate, resulted from the fluctuations in the oxygen concentration. For this purpose, CeO_2–CuO (CC) mixed metal oxide with enhanced oxygen storage capacity was synthesized via a coprecipitation method. The prepared mixed metal oxides were immobilized on the electrode surface for the first time in the literature to enhance the amperometric performance of the sensor and eliminate the false results in oxygen-lean environments by exploiting their high redox properties. The performance of the constructed Pt/CC/LOx sensors was compared with pristine ceria containing (Pt/CeO_2/LOx) and ceria-free (Pt/LOx) sensors. The use of CeO_2–CuO mixed metal oxide, which had much higher OSC than pristine ceria, acted as an oxygen buffer on the sensing platform in oxygen-depleted buffer solution. Thus, the false results associated with the depletion of oxygen tension in PBS solution were eliminated. On the other hand,

Table 4
Comparison of the performance of the proposed sensor with various lactate biosensors.

Sensor	Sensitivity (μA mM^{-1} cm^{-2})	Linear range (mM)	LOD (μM)	Ref.
LOx/DNPs/Au	4.0	0.05–0.7	15	[38]
LOx/ZnO-NRs/Au/Glass	N/A	0.1–1	0.1	[39]
LOx/DTSP/Au	1.49	up to 1.2	14	[40]
Nafion/LOx/Au/ZnO	24.56	0.01–0.6	6	[41]
LOx/ZnO-NWRs	15.6	0.012–1.2	12	[42]
Pt/CeO2-3(PEI/LOx)-3(PEI/AOx)	174.3	0.02–1	0.3	[33]
Nafion/LOx/CeO_2–CuO/Pt	89.3 ± 4	0.02–0.6	3.3	This work

DNPs: Diamond nanoparticles.
ZnO-NRs: ZnO nanorods.
DTSP: Dithiobos-N-succinimidyl propionate.
ZnO-NWRs: ZnO nanowires.
PEI: Polyethylenenimine.

Please cite this article in press as: A. Uzunoglu, L.A. Stanciu, Novel CeO_2–CuO-decorated enzymatic lactate biosensors operating in low oxygen environments, Analytica Chimica Acta (2016), http://dx.doi.org/10.1016/j.aca.2015.12.044

at relatively high lactate concentrations (larger than 200 μM) the reduction of metal oxide nanoparticles could not supply enough oxygen to sustain the enzymatic lactate reaction in O_2-lean conditions, which led to a deviation in the linearity of current vs. molarity graph. Our results showed that ceria-based materials with enhanced OSC can be used to construct amperometric lactate biosensors with high sensitivity, which are capable of working in O_2-lean conditions in the concentration range up to 0.2 μM. The constructed sensors showed good reliability and selectivity in human serum. Based on these results, we conclude that taking advantage of the oxygen storage properties of CeO_2–CuO particles can be a potential solution towards the fabrication of new sensors capable of the real-time monitoring of lactate levels.

Acknowledgements

The authors would like to acknowledge the financial support provided by NSF under Award No. CMMI 1200066.

Appendix A. Supplementary data

Supplementary data related to this article can be found at http://dx.doi.org/10.1016/j.aca.2015.12.044.

References

[1] J. Bakker, A.P. de Lima, Crit. Care 8 (2004) 96.
[2] M. Pagan, D. Suazo, N. del Toro, K. Griebenow, Biosens. Bioelectron. 64 (2015) 138.
[3] L. Rassaei, W. Olthuis, S. Tsujimura, E.J.R. Sudholter, A. van den Berg, Anal. Bioanal. Chem. 406 (2014) 123.
[4] M.M. Sayeed, P.N.A. Murthy, Circ. Shock 8 (1981) 657.
[5] J. Meakins, C.N.H. Long, J. Clin. Investig. 4 (1927) 273.
[6] N. Nikolaus, B. Strehlitz, Microchim. Acta 160 (2008) 15.
[7] W. Brinkert, J.H. Rommes, J. Bakker, Intensive Care Med. 25 (1999) 966.
[8] S. Perez, S. Sanchez, E. Fabregas, Electroanalysis 24 (2012) 967.
[9] N.G. Poulos, J.R. Hall, M.C. Leopold, Langmuir 31 (2015) 1547.
[10] S. Perez, E. Fabregas, Analyst 137 (2012) 3854.
[11] K.E. Toghill, R.G. Compton, Int. J. Electrochem. Sci. 5 (2010) 1246.
[12] J. Wang, Chem. Rev. 108 (2008) 814.
[13] D.A. Gough, J.Y. Lucisano, P.H.S. Tse, Anal. Chem. 57 (1985) 2351.
[14] G. Reach, G.S. Wilson, Anal. Chem. 64 (1992) A381.
[15] J. Wang, F. Lu, J. Am. Chem. Soc. 120 (1998) 1048.
[16] M.G. Loughran, J.M. Hall, A.P.F. Turner, Electroanalysis 8 (1996) 870.
[17] A. Chaubey, B.D. Malhotra, Biosens. Bioelectron. 17 (2002) 441.
[18] J. Njagi, C. Ispas, S. Andreescu, Anal. Chem. 80 (2008) 7266.
[19] C.W. Sun, H. Li, L.Q. Chen, Energy Environ. Sci. 5 (2012) 8475.
[20] A. Kolmakov, M. Moskovits, Annu. Rev. Mater. Res. 34 (2004) 151.
[21] P.R. Solanki, A. Kaushik, V.V. Agrawal, B.D. Malhotra, Npg Asia Mater. 3 (2011) 17.
[22] N. Tsud, R.G. Acres, M. Iakhnenko, D. Mazur, K.C. Prince, V. Matolin, J. Phys. Chem. B 117 (2013) 9182.
[23] E.P. Murray, T. Tsai, S.A. Barnett, Nature 400 (1999) 649.
[24] H.J. Beie, A. Gnorich, Sens. Actuators B Chem. 4 (1991) 393.
[25] M. Stoukides, Catal. Rev. Sci. Eng. 42 (2000) 1.
[26] S. Armini, J. De Messemaeker, C.M. Whelan, M. Moinpour, K. Maex, J. Electrochem. Soc. 155 (2008) H653.
[27] T. Morimoto, H. Tomonaga, A. Mitani, Thin Solid Films 351 (1999) 61.
[28] A. Asati, S. Santra, C. Kaittanis, S. Nath, J.M. Perez, Angew. Chemie Int. Ed. 48 (2009) 2308.
[29] J.D. Qiu, S.G. Cui, R.P. Liang, Microchim. Acta 171 (2010) 333.
[30] A. Trovarelli, Catal. Rev. Sci. Eng. 38 (1996) 439.
[31] A. Uzunoglu, H. Zhang, S. Andreescu, S. Stanciu, Springer, J. Mater. Sci. (2015) 3750.
[32] G.L. Zhou, H. Lan, X.Q. Yang, Q.X. Du, H.M. Xie, M. Fu, Ceram. Int. 39 (2013) 3677.
[33] A. Uzunoglu, I. Ramirez, E. Andreasen, L. Stanciu, Manuscript Submitted for Publication.
[34] R.E. Ozel, C. Ispas, M. Ganesana, J.C. Leiter, S. Andreescu, Biosens. Bioelectron. 52 (2014) 397.
[35] N.P. Sardesai, A. Karimi, S. Andreescu, Chemelectrochem 1 (2014) 2082.
[36] A. Uzunoglu, A.D. Scherbarth, L. Stanciu, Sens. Actuators B Chem. (2015) 968.
[37] D.T. Burns, K. Danzer, A. Townshend, Pure Appl. Chem. 74 (2002) 2201.
[38] M. Briones, E. Casero, M.D. Petit-Dominguez, M.A. Ruiz, A.M. Parra-Alframba, F. Pariente, E. Lorenzo, L. Vazquez, Biosens. Bioelectron. 68 (2015) 521.
[39] Z.H. Ibupoto, S. Shah, K. Khun, M. Willander, Sensors 12 (2012) 2456.
[40] M. Gamero, F. Pariente, E. Lorenzo, C. Alonso, Biosens. Bioelectron. 25 (2010) 2038.
[41] Y. Zhao, X. Fang, Y. Gu, X. Yan, Z. Kang, X. Zheng, P. Lin, L. Zhao, Y. Zhang, Colloids Surf. B Biointerfaces 126 (2015) 476.
[42] Y.G. Zhao, X.Q. Yan, Z. Kang, X.F. Fang, X. Zheng, L.Q. Zhao, H.W. Du, Y. Zhang, J. Nanoparticle Res. 16 (2014) 9.

Please cite this article in press as: A. Uzunoglu, L.A. Stanciu, Novel CeO_2–CuO-decorated enzymatic lactate biosensors operating in low oxygen environments, Analytica Chimica Acta (2016), http://dx.doi.org/10.1016/j.aca.2015.12.044